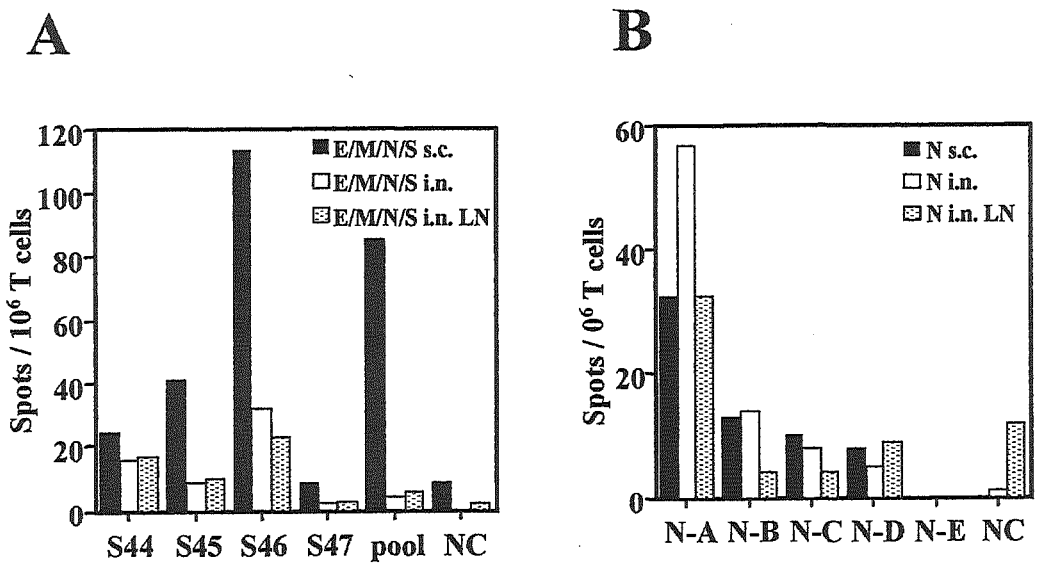
A
B
120
100
80
60
40
20
0
Spots / 10^6 T cells
E/M/N/S s.c.
E/M/N/S i.n.
E/M/N/S i.n. LN
S44
S45
S46
S47
pool
NC
60
40
20
0
Spots / 0^6 T cells
N s.c.
N i.n.
N i.n. LN
N-A
N-B
N-C
N-D
N-E
NC

Fig.6

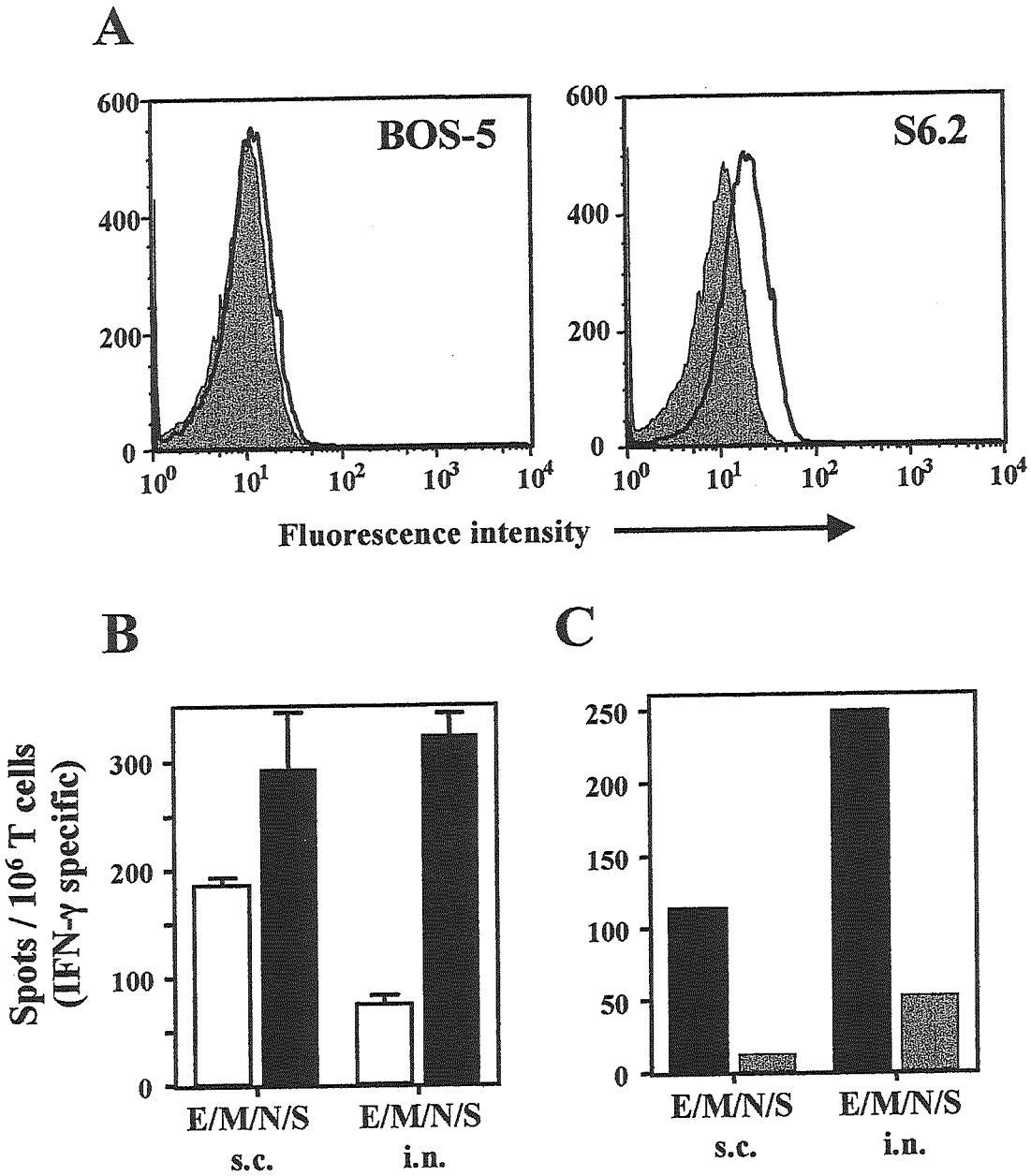
A
BOS-5
S6.2
600
400
200
0
10^0
10^1
10^2
10^3
10^4
Fluorescence intensity
B
C
Spots / 10^6 T cells
(IFN-γ specific)
300
200
100
250
150
50
E/M/N/S
s.c.
E/M/N/S
i.n.

Fig.7

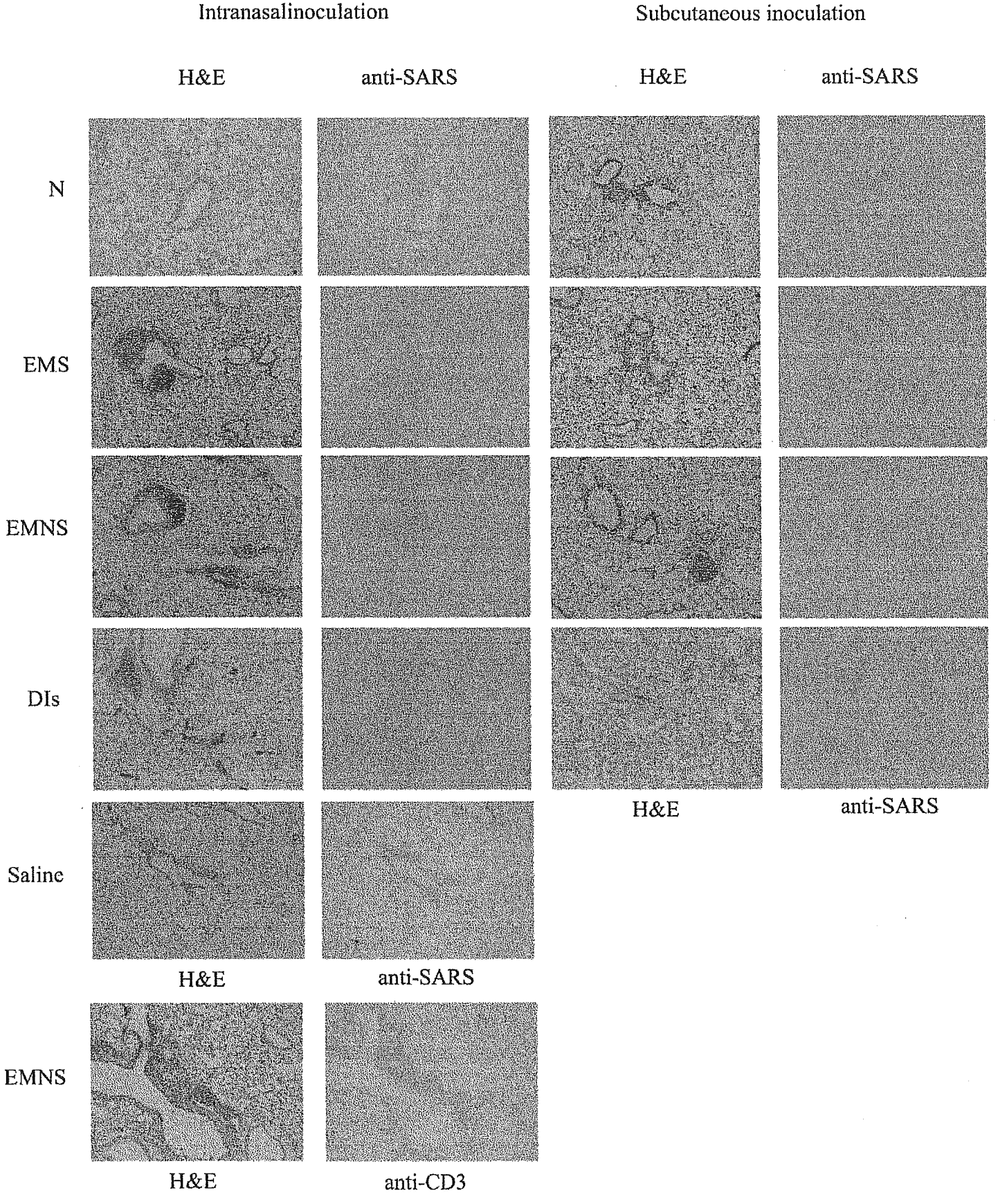
Intranasalinoculation
Subcutaneous inoculation
H&E
anti-SARS
H&E
anti-SARS
N
EMS
EMNS
DIs
H&E
anti-SARS
Saline
H&E
anti-SARS
EMNS
H&E
anti-CD3

Fig.8

Table 1. Titers of SARS-CoV specific and neutralizing antibodies

	i.n.		s.c.	
	[a]SARS-specific IgG titer (ELISA units/ml)	[b]Neutralization antibody titer	[a]SARS-specific IgG titer (ELISA units/ml)	[b]Neutralization antibody titer
rDIsSARS-M	488	n.d.	22296	n.d.
	388	n.d.	5147	n.d.
	606	n.d.	12395	n.d.
	556	n.d.	8398	n.d.
rDIsSARS-N	1560	n.d.	5931	n.d.
	2279	n.d.	4855	n.d.
	10630	n.d.	8890	n.d.
	2906	n.d.	1451	n.d.
rDIsSARS-S	5984	x300	4768	x300
	7852	x1500	13390	x1500
	1679	x60	807	x300
	33113	x1500	3467	x1500
rDIsSARS-E/M/S	6465	x60	13385	x60
	5779	x60	9225	x60
	2489	x60	25099	x60
	3165	n.d.	36708	x1500
rDIsSARS-E/M/N/S	9964	x60	58522	x1500
	8266	x300	19683	x300
	20188	x1500	15410	x300
	5154	x60	26550	x1500
DIs	212	n.d.	1824	n.d.
	922	n.d.	2583	n.d.
	214	n.d.	1066	n.d.
	394	n.d.	1441	n.d.

n.d. not detected

[a]SARS-CoV-specific IgG titers were calculated as described in Fig.3.
[b]Neutralization antibody titers were expressed as the minimal dilutions of serum capable of inhibiting the cytopathic effects of the virus.

Jpn. J. Infect. Dis., 58, 88-94, 2005

Original Article

Immunological Detection of Severe Acute Respiratory Syndrome Coronavirus by Monoclonal Antibodies

Kazuo Ohnishi, Masahiro Sakaguchi, Tomohiro Kaji, Kiyoko Akagawa, Tadayoshi Taniyama, Masataka Kasai, Yasuko Tsunetsugu-Yokota, Masamichi Oshima, Kiichi Yamamoto, Naomi Takasuka, Shu-ichi Hashimoto, Manabu Ato, Hideki Fujii, Yoshimasa Takahashi, Shigeru Morikawa[1], Koji Ishii[2], Tetsutaro Sata[4], Hirotaka Takagi[5], Shigeyuki Itamura[3], Takato Odagiri[3], Tatsuo Miyamura[2], Ichiro Kurane[1], Masato Tashiro[3], Takeshi Kurata[6], Hiroshi Yoshikura[6] and Toshitada Takemori*

Department of Immunology, [1]Department of Virology I, [2]Department of Virology II, [3]Department of Virology III, [4]Department of Pathology and [5]Division of Biosafety Control and Research, [6]National Institute of Infectious Diseases, Tokyo 162-8640, Japan

(Received October 20, 2004. Accepted February 14, 2005)

SUMMARY: In order to establish immunological detection methods for severe acute respiratory syndrome coronavirus (SARS-CoV), we established monoclonal antibodies directed against structural components of the virus. B cell hybridomas were generated from mice that were hyper-immunized with inactivated SARS-CoV virion. By screening 2,880 generated hybridomas, we established three hybridoma clones that secreted antibodies specific for nucleocapsid protein (N) and 27 clones that secreted antibodies specific for spike protein (S). Among these, four S-protein specific antibodies had in vitro neutralization activity against SARS-CoV infection. These monoclonal antibodies enabled the immunological detection of SARS-CoV by immunofluorescence staining, Western blot or immunohistology. Furthermore, a combination of monoclonal antibodies with different specificities allowed the establishment of a highly sensitive antigen-capture sandwich ELISA system. These monoclonal antibodies would be a useful tool for rapid and specific diagnosis of SARS and also for possible antibody-based treatment of the disease.

INTRODUCTION

The outbreak of severe acute respiratory syndrome (SARS) in 2003, caused by SARS coronavirus (SARS-CoV)(1,2), ultimately led to 8,000 people becoming infected, 916 of whom died (3; http://who.int/csr/sars/country/en/country2003_08_15.pdf). Even though the WHO announced an end to the epidemic (4; http://www.who.int/entity/csr/sars/resources/en/SARSReferenceLab1.pdf), the threat of re-emergence persists due to the absence of a vaccine, and inability of health services to rapidly detect and specifically diagnose the disease. One of the critical issues in the management of clinical patients and control of the pandemic is a system of early diagnosis that distinguishes SARS from other types of pulmonary infections. As an epidemiological history of contact with SARS patients is not always provable and there are no clinical signs unique to SARS patients (5), confirmatory diagnosis relies primarily on laboratory tests.

To date, viral shedding of SARS-CoV has been extensively studied to improve diagnosis and infectious control (6-8). Maximum virus shedding takes place between day 12 and day 14 of disease onset. For most acute respiratory viral infections, viral shedding occurs within the first few days from the nasopharyngeal tissue and soon after at the upper respiratory tract, but seldom lasts for more than 10 days (6-8). The peak of shedding in stools occurs a few days after respiratory shedding and remains high even after 3 weeks (7, 8). SARS-CoV was detected in patients' plasma samples within several days of the onset of fever, sometimes at levels equivalent to those recorded for nasopharyngeal aspirates (6, 9).

Previously, during the outbreak in Hong Kong (8), laboratory diagnosis for SARS virus infection was based on a combination of serologic tests, reverse transcription-polymerase chain reaction (RT-PCR), and virus isolation. IgG seroconversion among those infected was 93% by day 28 (5), suggesting that while antibody seroconversion provides reliable proof of infection (5,10); it is, however, not suitable for early diagnosis (11). Among patients in whom the serological evidence could be retrospectively examined, RT-PCR provided about 60% of the diagnostic yield using tracheal aspirates and stools for the first 2 weeks after the onset of illness (8). Although the availability of data that compares the diagnostic yield of various specimen types is still limited, it has been suggested that a combination of stool samples and pooled throat and nasal swab specimens provides reagents for safe and high-yield SARS-CoV detection (8). Furthermore, in addition to RT-PCR on respiratory and fecal samples, serology is needed to confirm the diagnosis of SARS-CoV infection in most cases.

Based on clinical experience, several options have been considered in the quest to develop the capacity to accurately diagnose SARS-CoV infection, including molecular biology techniques and serological tests such as antigen-captured ELISA assay and immunofluorescence assay to detect virus-infected cells in respiratory swabs (5-12). The preparation of monoclonal antibodies (mAbs) is considered to be valuable especially for serological testing.

*Corresponding author: Mailing address: Department of Immunology, National Institute of Infectious Diseases, Toyama 1-23-1, Shinjuku-ku, Tokyo 162-8640, Japan. Tel: +81-3-5285-1111, Fax: +81-5285-1150, E-mail: ttoshi@nih.go.jp

In this paper we report the successful establishment and the characterization of mAbs against SARS-CoV structural components. These mAbs enabled the general immunological detection of SARS-CoV, by the methods such as immunofluorescent staining, Western blotting, and immunohistology, in addition to the construction of highly sensitive antigen-capture sandwich ELISA.

MATERIALS AND METHODS

Virus and cell culture: SARS-CoV (HKU-39849) was kindly supplied by Dr. J. S. M. Peiris, Department of Microbiology, the University of Hong Kong. The live virus was manipulated under the physical containment level P3. For the purification of the virion, the day-2 culture supernatant of Vero E6, which had been infected with SARS-CoV at moi = 1.0, was centrifuged at 8,000×g for 30 min to remove cell debris. The virion in the supernatant was precipitated with 8% polyethylene glycol/ 0.5 M NaCl, and further purified by 20%/60%-discontinuous sucrose density gradient centrifugation. This fraction was inactivated by UV-irradiation (260 nm, 4.75 J/cm^2), and used as UV-inactivated SARS-CoV fraction. We and others confirmed that this condition completely inactivates SARS-CoV (13,14).

Production of mAbs: BALB/c mice (9-week old females, Japan SLC) were immunized subcutaneously with 20 μg of UV-inactivated SARS-CoV using Freund's Complete Adjuvant (FCA, Sigma, St. Louis, Mo., USA). After 2 weeks, the mice were boosted with a subcutaneous injection of 5 μg of UV-inactivated SARS-CoV using Freund's Incomplete Adjuvant (FIA, Sigma). On day-3 after the boost, sera from the mice were tested by ELISA for the antibody titer against SARS-CoV. The two mice showing highest antibody titer were further boosted intravenously with 5 μg of the inactivated virus 14 days after the previous boost. This immunization schedule was called protocol-1. In protocol-2 the booster injection was repeated two more times before the final boost. Three days after the final boost, spleens from two mice were excised and the splenocytes were fused with Sp2/O-Ag14 myeloma by the polyethylene glycol method of Kozbor and Roder (15). The fused cells from the two spleens were cultured and HAT-selected on twenty 96-well plates. The first screening was conducted by ELISA using SARS-CoV infected Vero E6 cell lysate as the antigen. In this first screening, the ELISA with uninfected Vero E6 cell lysate was used as the negative control. After the virus was inactivated by UV-irradiation, cell lysates were prepared by NP-40 lysis buffer (1% NP-40/ 150 mM NaCl/ 50 mM Tris, pH 7.5) followed by centrifugation at 15,000 rpm for 20 min to remove the cell debris. The supernatant was diluted 100-fold using ELISA-coating buffer (50 mM sodium bicarbonate, pH 9.6) and the ELISA plates (Dynatech, Chantily, Va., USA) were coated at 4°C overnight. After blocking with 1% ovalbumin in PBS-Tween (10 mM phosphate buffer, 140 mM NaCl, 0.05% Tween 20, pH 7.5) for 1 h, the culture supernatants from HAT-selected hybridomas were added and incubated for 1 h. After washing with PBS-Tween, the bound antibodies were detected with alkaline phosphatase-conjugated anti-mouse IgG (1:2000, Zymed, South San Francisco, Calif., USA) using *p*-nitrophenyl phosphate (PNPP) as a substrate. The second screening was conducted by ELISA using the cell lysates of chick embryonic fibroblast (CEF) cell lines that were transfected by vaccinia virus vector containing the gene either of SARS-CoV spike (S) or nucleocapsid (N) proteins.

Recombinant virus proteins: Genomic RNA was extracted from SARS-CoV strain HKU39849 and reverse transcribed to cDNA. The corresponding open reading frames (ORF) to E, M, N and S were amplified by PCR and cloned into the transfer vector, pDIsgptmH5, which also harbored *Escherichia coli* xantine-guanine phosphoribosyltransferase under the control of vaccinia virus p7.5 promoter in the cloning site of pUc/DIs (16). The recombinant clones of attenuated vaccinia virus, DIs, which harbored each ORF were obtained by homologous recombination induced in DIs-infected-, pDIsgptmH5-transfected CEF cells. The detailed protocol will be published elsewhere.

Neutralization assay: The known tissue culture infectious dose (TCID) of SARS-CoV was incubated for 1 h in the presence or absence of the purified mAbs serially diluted 10-fold, and then added to Vero E6 cell culture grown to confluence in a 96-well microtiter plate. As a control, mAbs against N protein was added to the culture. After 48 hr, cells were fixed with 10% formaldehyde and stained with crystal violet to visualize the cytopathic effect induced by the virus (17). Neutralization antibody titers were expressed as the minimum concentration of purified immunoglobulin that inhibits cytopathic effect.

Western blot: UV-inactivated purified SARS-CoV virion (0.5 μg/lane)(13) was loaded on SDS-PAGE under reduced conditions. Proteins were transferred to the PVDF membrane (Genetics, Tokyo, Japan). After blocking with BlockAce (Snow Brand Milk Products Co., Ltd., Tokyo, Japan) reagent, the membranes were reacted with the mAbs or the diluted sera (1:1000) that had been obtained from mice inoculated with UV-irradiated SARS-CoV. After washing, the membrane was reacted with peroxidase-conjugated F(ab')$_2$ fragment anti-mouse IgG (H+L) (1:20,000 Jackson Immuno Research, West Grove, Pa., USA), and the bands were visualized using chemiluminescent reagents (Amasham Biosciences, Piscataway, N.J., USA) on the X-ray film (Kodak, Rochester, N.Y., USA).

Purification and biotinylation of mAbs: Hybridomas were grown in Hybridoma-SFM medium (Invitrogen, Carlsbad, Calif., USA) supplemented with recombinant IL-6 (18) and penicillin (100 U/mL)/streptomycin (100 μg/mL). The culture supernatants were harvested, added with 1/100 volume of 1 M Tris-HCl (pH 7.4) and 1/500 volume of 10% NaN_3, and directly loaded on the Protein G-Sepharose 6B column (Amersham Biosciences). The column was washed with PBS and eluted with Glycine/HCl (pH 2.8). After measuring the OD_{280} of the fractions, protein containing fractions were pooled and added with an equal volume of saturated $(NH_4)_2SO_4$. Precipitated proteins were dissolved in PBS, dialysed against PBS and stored at −20°C. The purified antibodies were biotinylated using sulfo-NHS-LC-biotin (Pierce, Rockford, Ill., USA) according to the manufacturer's protocol.

Antigen-capture ELISA: The purified mAb for the antigen-capture was immobilized on the microplate (Immulon 2, Dynatech) by incubating 4 μg/mL antibody in 50 mM sodium bicarbonate buffer (pH 8.6) at 4°C overnight. The microplate was blocked with 1% BSA, washed with PBS-Tween, and reacted with serial dilution of UV-inactivated purified SARS-CoV for 1 h at room temperature. After washing with PBS-Tween, wells were reacted with biotinylated probing mAb (0.1 μg/mL) for 1 h at room temperature. After washing, wells were reacted with β-D-galactosidase-labeled streptavidine (Zymed) for 1 h at room temperature. After washing,

fluorescent substrate 4-methylumberyferyl-β-D-galactoside (Sigma-Aldrich, St. Louis, Mo., USA) was added and the substrate was incubated for 2 h at 37°C. The reaction was stopped by adding 0.1M Glycine-NaOH (pH 10.2) and the fluorescence (FU) of the reaction product, 4-methylumberiferron, was measured using FluoroScan (Flow Laboratories Inc., Inglewood, Calif., USA).

Histology: Formaldehyde-fixed human lung tissue that was RT-PCR positive for SARS-CoV (19) and lung from a SARS-CoV infected macaque were embedded in paraffin and sectioned using the standard method. After de-paraffinization by standard method, the sections were soaked with 0.1 M citrate-buffer (pH 6.0) and autoclaved for 10 min at 121°C to inactivate viruses. Endogenous peroxidase was inactivated by 0.3% hydrogen peroxide for 30 min at room temperature. After blocking with 5% normal goat serum for 10 min, sections were incubated with the mAb at 4°C overnight. The bound antibody was detected by biotinylated anti-mouse IgG followed by peroxidase-labeled streptavidin (LSAB2 kit, DakoCytomation, Kyoto, Japan) and visualized with 0.2 mg/mL 3,3′-diaminobenzidine in 0.015% hydrogen peroxide/0.05M Tris-HCl (pH 7.6). The sections were counterstained with hematoxylin.

RESULTS

In order to establish the hybridomas that secrete specific mAbs to SARS-CoV, we immunized BALB/c mice with purified SARS-CoV whole virion fraction. The virus was inactivated by UV-irradiation to avoid a change in antigenicity presumably caused by aldehyde-fixation or detergent-solubilization. The immunization protocols used were those of the standard method in which the boost administrations were repeated twice (protocol-1) or four times (protocol-2) with 2-week intervals using FCA/FIA as an adjuvant (see Materials and Methods). Three days after the final boost, a single cell suspension was prepared from two spleens of immunized mice and fused with SP-2/O myeloma by a polyethylene-glycol method, the fused cells were then HAT-selected (15).

In the experiment with immunization protocol-1, we found that the culture supernatants from 28 of the 1,920 wells were strong-positive in ELISA testing in which the cell-lysate of SARS-CoV infected Vero E6 cells was used as a coated antigen (Table 1). As a negative control, we used uninfected Vero E6 cell-lysate as the antigen. Wells that showed a positive reaction were omitted from the count. Among the 28 wells, 19 reacted to vaccinia vector-based recombinant-S-protein and three reacted to recombinant-N-protein. These hybridomas were successfully cloned by a repeated limiting dilution method. The remaining six wells did not give rise to a significant positive signal to recombinant-S, -N or -M proteins. One anti-S mAb cross-reacted to porcine transmissible gastroenteritis virus (TGEV) and this clone was also omitted from further studies. None of these mAbs cross-reacted to mouse hepatitis virus (MHV).

The avidities of these cloned mAbs were tested by avidity-ELISA in the presence of urea. Although in the presence of 6 M urea some anti-S mAbs retained 18-35% of the original reactivity, less than 10% of the original reactivity remained in the presence of 8 M urea (Table 2). Three anti-N mAbs showed a very low avidity index in this assay system.

In a previous report that studied human IgG avidity maturation after rubella vaccination, high-avidity antibodies were defined as those that retain more than 50% of reactivity in the presence of 8 M urea (20). Although it would not be possible to directly apply this definition of polyclonal antibodies to our mAb case, the avidities of mAbs we obtained did not seem particularly high. This prompted us to attempt to obtain better mAbs with higher avidity by repeating booster immunization in anticipation of affinity maturation. After an additional two boosts, hybridomas were established by the same procedure as the first experiment. We screened 960 wells and obtained 14 wells positive for ELISA with SARS-CoV infected Vero E6 cell lysate (Table 1). Among the 14 wells, seven reacted with recombinant-S protein and none of them reacted with recombinant-N or -M proteins. These anti-S antibodies showed significantly higher avidity in the avidity ELISA (two representative clones are shown in Table 2). From the results of this avidity test, we selected five anti-S mAbs that showed the highest avidity index. None of these mAbs cross-reacted to human coronavirus, 229E (data not shown). These five anti-S and three anti-N mAbs were purified, and characterized further.

All selected mAbs worked successfully in the immunofluorescent staining assay (Fig. 1). Anti-S mAbs such as SKOT-3, -10, -20, SOAT-5 and -13 stained the Golgi body and surface membrane of virus-infected cells but not of uninfected-cells. In contrast, the staining patterns of anti-N mAbs such as SKOT-7, -8 and -9 were mainly confined to the Golgi body.

All anti-N mAbs worked in immunohistochemistry of formalin-fixed, paraffin-embedded sections of both human lung from SARS patients and SARS-CoV infected macaque lung (Fig. 2). The specificity of these stainings was confirmed by the negative results for normal lungs and several specimens from pneumonia patients including cases complicated by measles, influenza type A, herpes-simplex and herpes zoster.

The mAbs that worked for immunohistochemistry, i.e.,

Table 1. Summary of the first hybridoma screening by ELISA

Immobilized antigen	Experiment-1[1)]	Experiment-2[2)]	Total
(Total wells assayed)	1,920	960	2,880
SARS-CoV infected Vero cell-lysate	28	14	42
Recombinant - S	19	7	26
- N	3	0	3

[1)]: Immunization protocol-1
[2)]: Immunization protocol-2

Table 2. Avidity ELISA

Clone	Epitope	Avidity Index (%)		
		4M urea	6M urea	8M urea
Experiment-1				
SKOT-7	N	1.6	1.2	1.5
SKOT-8	N	2.3	3.2	3.7
SKOT-9	N			
SKOT-3	S	45.5	18.7	1.2
SKOT-10	S	73.4	29.9	2.6
SKOT-20	S	63.8	35.4	8.8
Experiment-2				
SOAT-5	S	51.3	48.0	43.3
SOAT-13	S	77.0	62.0	48.0

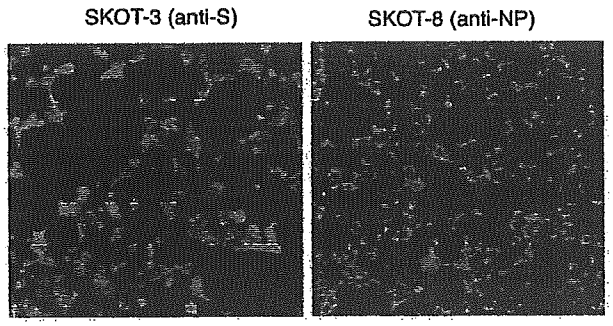

Fig. 1. Fluorescent immunostaining of SARS-CoV infected Vero E6 cells with monoclonal antibodies (mAbs). Parformaldehyde-fixed, SARS-CoV infected Vero E6 cells were permeabilized with TBS-tween and incubated with mAbs from hybridoma clones and the antibodies were detected with FITC-conjugated anti-mouse IgG. Shown are representative staining patterns with anti-S mAb, SKOT-3 (A), and anti-N mAb, SKOT-8 (B).

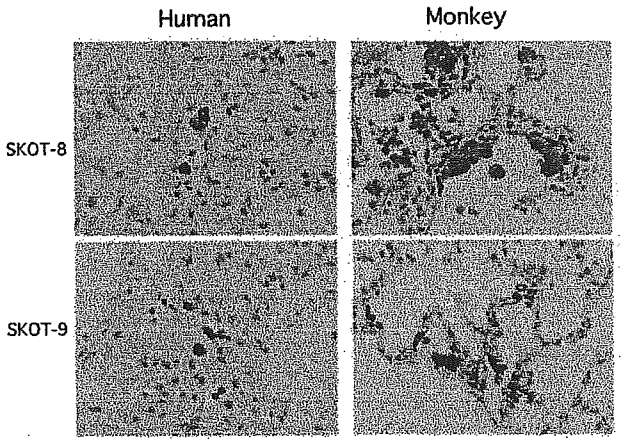

Fig. 2. Immuno-histochemistry of SARS-CoV infected human lung and macaque lung tissues with mAbs. Paraformaldehyde-fixed, paraffin-embedded sections were incubated with mAbs, and then with biotinylated anti-mouse IgG/peroxidase-labeled streptavidin complex before being visualized using DAB as a peroxidase substrate. Counter-staining with hematoxilin. Shown are human patient lung tissue (left panels) and SARS-infected macaque lung tissues (right panels), stained with anti-N mAbs (SKOT-8, SKOT-9).

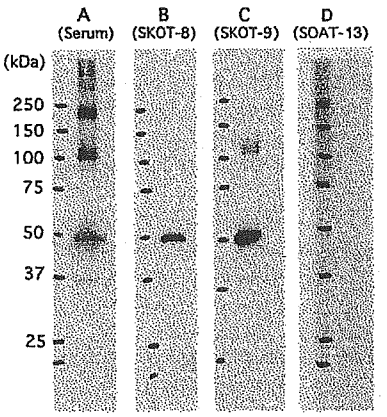

Fig. 3. Detection of virus proteins with Western blot. Purified SARS-CoV proteins (0.5 μg/lane) were electrophoresed with SDS-PAGE under reducing conditions. After blotting on the PVDF membrane, proteins were detected by incubation with mAbs, followed by incubation with peroxidase labeled-F(ab')$_2$ fragment of Donkey anti-mouse IgG. They were then visualized by chemiluminescent reaction. A: mouse serum from SARS-CoV immunized mouse; B: anti-N mAb, SKOT-8; C: anti-N mAb, SKOT-9; D: anti-S mAb, SOAT-13. The positions of molecular weight markers are shown on the left.

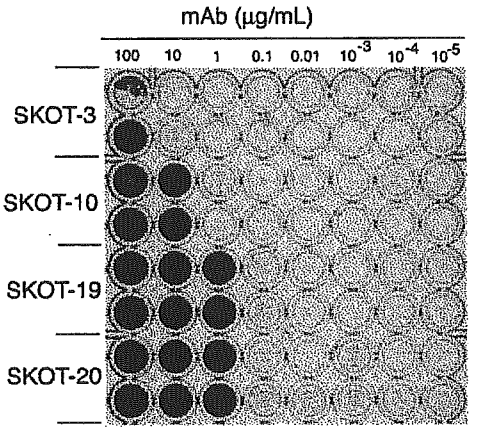

Fig. 4. In vitro neutralization assay of SARS-CoV infection with mAbs. Purified SARS-CoV fraction was diluted to 1×10^2 PFU/mL and incubated with serially-titrated purified mAbs for 1 h at 37°C. After the reaction, samples were poured into wells of a 96-well plate on which Vero E6 cells were grown to 90% confluent. After 48 h, cytotoxicities were visualized by staining the cells with crystalviolet. The results of purified anti-S antibodies (SKOT-3, -10, -19 and -20) with concentrations ranging from 100 μg/mL to 10^{-5} μg/mL are shown.

SKOT-7, -8 and -9 also worked for Western-blot detection of the viral proteins (Fig. 3). Anti-N mAbs detected a band of 50 kDa that corresponds to the calculated molecular weight of SARS-CoV N-protein. In some experiments with longer exposure, a band with an apparent molecular weight of 120 kDa was also detected. None of the anti-S mAbs worked in the Western blot, suggesting that the major antigenic determinants of the S-protein are 'conformational' epitopes.

We tested the in vitro neutralizing activities of anti-S mAbs. As shown in Fig. 4, SKOT-20 neutralized in vitro SARS-CoV infection to Vero E6 cells at an antibody concentration of 1 μg/mL. Another anti-S mAb, SKOT-19, which had a low avidity value, also showed similar neutralizing activity. SKOT-10 and -3 also had neutralization activity but required higher antibody concentrations.

Lastly, we tried to construct an antigen-capture detection system for SARS-CoV by sandwich ELISA. In preliminary experiments, we tested all the combinations of two mAbs from the selected eight mAbs to obtain the highest detection sensitivity for purified SARS-CoV virion, and found that the immobilization of SKOT-8 on the ELISA plate followed by the detection with biotinylated SKOT-9 gave the best result (data not shown; see Materials and Methods). In this sandwich ELISA, SARS-CoV protein was successfully detected in a concentration as low as 40 pg/mL (Fig. 5). Since the mAbs were originally raised against SARS-CoV strain HKU39849, we tested the validity of this system for other strains of SARS-CoV. As shown in Fig. 6, it was confirmed that the strains HK14T1WL, CDC00592 and Frankfurt1 were as detectable as HKU39849 using this system.

DISCUSSION

We established mAbs against SARS-CoV, which enable

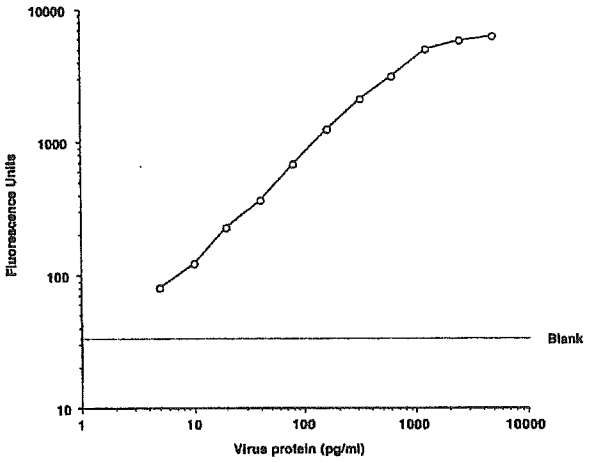

Fig. 5. Antigen-capture ELISA of SARS-CoV with mAbs. Anti-N mAb, SKOT-8, was immobilized on the surface of a 96 well plate. Serially-titrated purified SARS-CoV fractions were reacted for 1 h at room temperature and the bound virus proteins were detected by biotinylated SKOT-9 (anti-N) antibody followed by peroxydase-labeled streptavidin. They were then quantitated by chemiluminescent reaction using 4-methylumberiferril as a substrate. Abscissa: concentration of purified SARS-CoV proteins; ordinate: fluorescent unit.

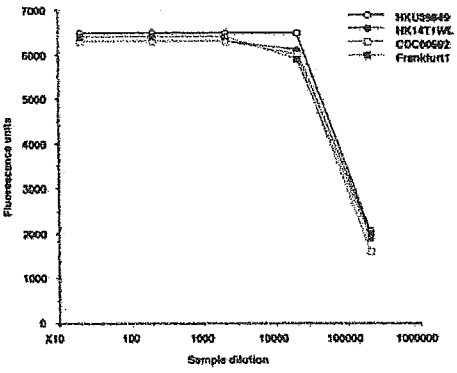

Fig. 6. Comparison of SARS-CoV strains for reactivity to the antigen capture sandwich ELISA. SARS-CoV strains, HKU39849, HK14T1WL, CDC00592 and Frankfurt1 were tested for the reactivity to the antigen-capture ELISA system as described in Fig. 5. Abscissa: sample dilution; ordinate: fluorescent units.

the detection of virus S- and N-proteins by means of immunofluorescence assay, immunohistochemistry, Western blot and antigen-capture ELISA. A summary of selected mAbs is shown in Table 3.

Among the originally selected 42 mAbs that were positive in ELISA for SARS-CoV infected Vero E6 cell lysate, 26 reacted to recombinant-S-protein and only three reacted to N-protein. We could not find hybridoma secreting mAb to M-protein or other protein components of SARS-CoV. These results suggest that S protein is the dominant target in the antibody response. We observed that none of the anti-S mAbs established worked in Western blot, suggesting that these mAbs may recognize 'conformational' epitopes. In contrast, all three anti-N mAbs worked in Western blot and immunohistochemistry, suggesting that these mAbs recognize 'linear' epitopes.

We examined whether our mAbs were applicable for immunofluorescence detection of virus-infected cells. In immunofluorescent staining of Vero E6 cells infected with SARS-CoV, anti-N mAbs stained the Golgi body and anti-S mAbs stained the Golgi body and surface membrane. This difference in localization of N- and S-proteins may reflect the common assembly process of coronaviruses (21). Further analysis is needed to clarify sensitivity and specificity in infected cells for clinical use.

During the course of outbreak of SARS-CoV in Hong Kong, it was reported that more than half the patients were not positively diagnosed by RT-PCR (8). Therefore, the diagnosis was finally confirmed by serum specimens in a convalescent-phase at a late stage of illness (8). To overcome this problem, virus shedding patterns have been extensively analyzed, with results showing that respiratory shedding of the virus increases over the first week and viral shedding in stools begins a few days after respiratory shedding (7,8). From this analysis, it is considered that a combination of stool sampling and pooled throat and nasal swab specimens could be good specimens for safe and highly sensitive SARS-CoV detection.

In general, a single diagnostic test is not conclusively reliable, because of the serious potential for false positives and negatives. Considering the limited sensitivity of RT-PCR, serological screening systems other than antibody detection are currently being examined (22,23). ELISA-based antigen captured assays are known to offer high specificity and reproducibility. Antigen-captured assays have been used in the diagnosis and monitoring of disease in cases of infection with dengue virus (24), human immunodeficient virus p24 (25) and Ebola hemorragic fever (26) and examined in hepatitis B virus and hepatitis C virus (22,23). In this context, extensive analysis in Ebola hemorragic fever suggests that the RT-PCR assay is extremely useful, but should always be utilized in combination with antigen-captured ELISA, which makes the diagnosis more reliable (26).

Table 3. Summary of selected hybridoma clones

Clone	Epitope	Class	IFA	Neutralization[1)]	Western-blot	Histology	Avidity (%)[2)]
SKOT-7	N	IgG	Golgi	-	50kDa	-	1.2
SKOT-8	N	IgG	Golgi	-	50kDa	Usable	3.2
SKOT-9	N	IgG	Golgi	-	120, 50kDa	Usable	3.8
SKOT-3	S	IgG	Golgi / cell membrane	100	-	-	18.7
SKOT-10	S	IgG	Golgi / cell membrane	10	-	-	29.9
SKOT-19	S	IgG	Golgi / cell membrane	1	ND	ND	ND
SKOT-20	S	IgG	Golgi / cell membrane	1	-	-	35.4
SOAT-5	S	IgG	Golgi / cell membrane	ND	-	-	48.0
SOAT-13	S	IgG	Golgi / cell membrane	ND	-	-	62.0

[1)]: Numbers represent minimum concentration (μg/mL) that exerts neutralization. -, no neutralization activity; ND, not determined.
[2)]: Avidity index at 6M urea (see Materials and Methods).

In the case of SARS-CoV, the assay has been recently evaluated by using mAbs and polyclonal antibodies directed against recombinant SARS-CoV nucleocapsid protein (22,23). A soluble N-protein was observed to be released from infected cells in culture, which led to the opportunity to evaluate the level in serum specimens from infected patients. N-antigen ELISA employing mAbs reproducibly detected 50% of patients on days 3 and 5 after the onset of illness, with a limitation of the detection of the recombinant protein at 50 pg/ml (22). N-antigen ELISA with use of polyclonal antibodies detected 60-50% of nasopharyngeal aspirate and fecal specimens from patients at day 3 to day 24 after the onset of illness, although the signal was relatively weak in fecal samples (22). These results suggest that antigen-captured assay could be useful for the early diagnosis of SARS-CoV infection.

We developed an antigen-capture ELISA system that detects purified SARS-CoV virion at levels as low as 40 pg/mL. The sensitivity of the system, which comprised two anti-N mAbs, seems high enough to detect virus protein in patient sera when compared to a recently reported antigen-capture ELISA system, which detects 100 pg/mL of purified recombinant N protein, successfully determined the virus protein in patient sera (22). We are now improving the sensitivity of the system and checking its applicability in the diagnosis and monitoring of SARS-CoV infection. Although none of our mAbs cross-reacted to human or other animal coronaviruses (229E, TGEV and MHV) by ELISA, it is also important to define the specificity of these mAbs by other techniques such as Western blot and immunofluorescent staining. This issue is currently under investigation.

Two anti-S mAbs, SKOT-19 and -20 demonstrated significant virus neutralizing activity. It would be interesting to address whether these mAbs interfere with the binding of the virion to its recently reported receptor, ACE2 (27). If this were the case, the humanization of these mAbs by means of either CDR-grafting or mouse-human chimeric antibody would be of interest as a possible application for the therapeutic use of these mAbs.

ACKNOWLEDGMENTS

We are grateful to Ms. Sayuri Yamaguchi for her assistance in establishing hybridomas.

This work was supported by grant from the Ministry of Health, Labour and Welfare of Japan.

REFERENCES

1. Drosten, C., Gunther, S., Preiser, W., van der Werf, S., Brodt, H. R., Becker, S., Rabenau, H., Panning, M., Kolesnikova, L., Fouchier, R. A., Berger, A., Burguiere, A. M., Cinatl, J., Eickmann, M., Escriou, N., Grywna, K., Kramme, S., Manuguerra, J. C., Muller, S., Rickerts, V., Sturmer, M., Vieth, S., Klenk, H. D., Osterhaus, A. D., Schmitz, H. and Doerr, H. W. (2003): Identification of a novel coronavirus in patients with severe acute respiratory syndrome. N. Engl. J. Med., 348, 1967-1976.
2. Ksiazek, T. G., Erdman, D., Goldsmith, C. S., Zaki, S. R., Peret, T., Emery, S., Tong, S., Urbani, C., Comer, J. A., Lim, W., Rollin, P. E., Dowell, S. F., Ling, A. E., Humphrey, C. D., Shieh, W. J., Guarner, J., Paddock, C. D., Rota, P., Fields, B., DeRisi, J., Yang, J. Y., Cox, N., Hughes, J. M., LeDuc, J. W., Bellini, W. J. and Anderson, L. J. (2003): A novel coronavirus associated with severe acute respiratory syndrome. N. Engl. J. Med., 348, 1953-1966.
3. World Health Organization (2003): Summary table of SARS cases by country, 1 November 2002 - 7 August 2003.
4. World Health Organization: WHO SARS international reference and verification laboratory network: policy and procedures in the inter-epidemic period.
5. Peiris, J. S., Chu, C. M., Cheng, V. C., Chan, K. S., Hung, I. F., Poon, L. L., Law, K. I., Tang, B. S., Hon, T. Y., Chan, C. S., Chan, K. H., Ng, J. S., Zheng, B. J., Ng, W. L., Lai, R. W., Guan, Y. and Yuen, K. Y. (2003): Clinical progression and viral load in a community outbreak of coronavirus-associated SARS pneumonia: a prospective study. Lancet, 361, 1767-1772.
6. Grant, P. R., Garson, J. A., Tedder, R. S., Chan, P. K., Tam, J. S. and Sung, J. J. (2003): Detection of SARS coronavirus in plasma by real-time RT-PCR. N. Engl. J. Med., 349, 2468-2469.
7. Cheng, P. K., Wong, D. A., Tong, L. K., Ip, S. M., Lo, A. C., Lau, C. S., Yeung, E. Y. and Lim, W. W. (2004): Viral shedding patterns of coronavirus in patients with probable severe acute respiratory syndrome. Lancet, 363, 1699-1700.
8. Chan, P. K., To, W. K., Ng, K. C., Lam, R. K., Ng, T. K., Chan, R. C., Wu, A., Yu, W. C., Lee, N., Hui, D. S., Lai, S. T., Hon, E. K., Li, C. K., Sung, J. J. and Tam, J. S. (2004): Laboratory diagnosis of SARS. Emerg. Infect. Dis., 10, 825-831.
9. Poon, L. L., Wong, O. K., Chan, K. H., Luk, W., Yuen, K. Y., Peiris, J. S. and Guan, Y. (2003): Rapid diagnosis of a coronavirus associated with severe acute respiratory syndrome (SARS). Clin. Chem., 49, 953-955.
10. Chen, W., Xu, Z., Mu, J., Yang, L., Gan, H., Mu, F., Fan, B., He, B., Huang, S., You, B., Yang, Y., Tang, X., Qiu, L., Qiu, Y., Wen, J., Fang, J. and Wang, J. (2004): Antibody response and viraemia during the course of severe acute respiratory syndrome (SARS)-associated coronavirus infection. J. Med. Microbiol., 53, 435-438.
11. Nie, Y., Wang, G., Shi, X., Zhang, H., Qiu, Y., He, Z., Wang, W., Lian, G., Yin, X., Du, L., Ren, L., Wang, J., He, X., Li, T., Deng, H. and Ding, M. (2004): Neutralizing antibodies in patients with severe acute respiratory syndrome-associated coronavirus infection. J. Infect. Dis., 190, 1119-1126.
12. Wang, W. K., Chen, S. Y., Liu, I. J., Chen, Y. C., Chen, H. L., Yang, C. F., Chen, P. J., Yeh, S. H., Kao, C. L., Huang, L. M., Hsueh, P. R., Wang, J. T., Sheng, W. H., Fang, C. T., Hung, C. C., Hsieh, S. M., Su, C. P., Chiang, W. C., Yang, J. Y., Lin, J. H., Hsieh, S. C., Hu, H. P., Chiang, Y. P., Yang, P. C. and Chang, S. C. (2004): Detection of SARS-associated coronavirus in throat wash and saliva in early diagnosis. Emerg. Infect. Dis., 10, 1213-1219.
13. Takasuka, N., Fujii, H., Takahashi, Y., Kasai, M., Morikawa, S., Itamura, S., Ishii, K., Sakaguchi, M., Ohnishi, K., Ohshima, M., Hashimoto, S., Odagiri, T., Tashiro, M., Yoshikura, H., Takemori, T. and Tsunetsugu-Yokota, Y. (2004): A subcutaneously injected UV-inactivated SARS coronavirus vaccine elicits systemic humoral immunity in mice. Int. Immunol., 16, 1423-1430.
14. Darnell, M. E., Subbarao, K., Feinstone, S. M. and Taylor, D. R. (2004): Inactivation of the coronavirus that

induces severe acute respiratory syndrome, SARS-CoV. J. Virol. Methods, 121, 85-91.
15. Kozbor, D. and Roder, J. C. (1984): In vitro stimulated lymphocytes as a source of human hybridomas. Eur. J. Immunol., 14, 23-27.
16. Ishii, K., Ueda, Y., Matsuo, K., Matsuura, Y., Kitamura, T., Kato, K., Izumi, Y., Someya, K., Ohsu, T., Honda, M. and Miyamura, T. (2002): Structural analysis of vaccinia virus DIs strain: application as a new replication-deficient viral vector. Virology, 302, 433-444.
17. Storch, G. A. (2001): Diagnostic Virology. p. 493-531. *In* Knipe, D.M., Howley, P.M., (ed.), Fields Virology. 4th ed. Vol. 1. Lippincott Williams & Wilkins, Philadelphia.
18. Karasuyama, H., Rolink, A. and Melchers, F. (1993): A complex of glycoproteins is associated with VpreB/ lambda 5 surrogate light chain on the surface of mu heavy chain-negative early precursor B cell lines. J. Exp. Med., 178, 469-478.
19. Nakajima, N., Asahi-Ozaki, Y., Nagata, N., Sato, Y., Dizon, F., Paladin, F. J., Olveda, R. M., Odagiri, T., Tashiro, M. and Sata, T. (2003): SARS coronavirus-infected cells in lung detected by new in situ hybridization technique. Jpn. J. Infect. Dis., 56, 139-141.
20. Hedman, K., Hietala, J., Tiilikainen, A., Hartikainen-Sorri, A. L., Raiha, K., Suni, J., Vaananen, P. and Pietilainen, M. (1989): Maturation of immunoglobulin G avidity after rubella vaccination studied by an enzyme linked immunosorbent assay (avidity-ELISA) and by haemolysis typing. J. Med. Virol., 27, 293-298.
21. Lai, M. M. C. and Holmes, K. V. (2001): *Coronaviridae*: the viruses and their replication. *In* Knipe, D. M. and Howley, P. M. (ed.), Fields Virology. 4th ed. Vol. 1. Lippincott Williams & Wilkins, Philadelphia.
22. Che, X. Y., Qiu, L. W., Pan, Y. X., Wen, K., Hao, W., Zhang, L. Y., Wang, Y. D., Liao, Z. Y., Hua, X., Cheng, V. C. and Yuen, K. Y. (2004): Sensitive and specific monoclonal antibody-based capture enzyme immunoassay for detection of nucleocapsid antigen in sera from patients with severe acute respiratory syndrome. J. Clin. Microbiol., 42, 2629-2635.
23. Lau, S. K., Woo, P. C., Wong, B. H., Tsoi, H. W., Woo, G. K., Poon, R. W., Chan, K. H., Wei, W. I., Peiris, J. S. and Yuen, K. Y. (2004): Detection of severe acute respiratory syndrome (SARS) coronavirus nucleocapsid protein in SARS patients by enzyme-linked immunosorbent assay. J. Clin. Microbiol., 42, 2884-2889.
24. Young, P. R., Hilditch, P. A., Bletchly, C. and Halloran, W. (2000): An antigen capture enzyme-linked immunosorbent assay reveals high levels of the dengue virus protein NS1 in the sera of infected patients. J. Clin. Microbiol., 38, 1053-1057.
25. Sutthent, R., Gaudart, N., Chokpaibulkit, K., Tanliang, N., Kanoksinsombath, C. and Chaisilwatana, P. (2003): p24 Antigen detection assay modified with a booster step for diagnosis and monitoring of human immunodeficiency virus type 1 infection. J. Clin. Microbiol., 41, 1016-1022.
26. Towner, J. S., Rollin, P. E., Bausch, D. G., Sanchez, A., Crary, S. M., Vincent, M., Lee, W. F., Spiropoulou, C. F., Ksiazek, T. G., Lukwiya, M., Kaducu, F., Downing, R. and Nichol, S. T. (2004): Rapid diagnosis of Ebola hemorrhagic fever by reverse transcription-PCR in an outbreak setting and assessment of patient viral load as a predictor of outcome. J. Virol., 78, 4330-4341.
27. Li, W., Moore, M. J., Vasilieva, N., Sui, J., Wong, S. K., Berne, M. A., Somasundaran, M., Sullivan, J. L., Luzuriaga, K., Greenough, T. C., Choe, H. and Farzan, M. (2003): Angiotensin-converting enzyme 2 is a functional receptor for the SARS coronavirus. Nature, 426, 450-454.